C. R. Mecanique 342 (2014) 692–699

Contents lists available at ScienceDirect

Comptes Rendus Mecanique

www.sciencedirect.com

A modeling and vibration analysis of a piezoelectric micro-pump diaphragm

Samira Kaviani, Mohsen Bahrami *, Amir Monemian Esfahani, Behzad Parsi

Dept. of Mechanical Engineering, Amirkabir University of Technology (Tehran Polytechnic), Tehran, Iran

ARTICLE INFO

Article history:
Received 18 May 2013
Accepted 30 June 2014
Available online 30 July 2014

Keywords:
Piezoelectric micro-pump
Diaphragm
Vibration analysis
Micro-electromechanical system
Finite element analysis
Orthogonality

ABSTRACT

The vibration analysis of a micro-pump diaphragm is presented. A piezoelectric micro-pump is studied. For this purpose, a dynamic model of the micro-pump is derived. The micro-pump diaphragm is modeled as circular double membranes, a piezoelectric one as actuator and a silicon one for representing the membrane for pumping action. The damping effect of the fluid is introduced into the equations. Vibration analysis is established by explicitly solving the dynamic model. The natural frequencies and mode shapes are calculated. The orthogonality conditions of the system are discussed. To verify the results, the finite-element micro-pump model is developed in ANSYS software package. The results show that the two methods are well comparable.

1. Introduction

The emergence of micro-fabrication in the last decade has introduced new ways to miniaturize many devices. One of the important uses of this technology is in drug-delivery systems. Some diseases respond differently according to the drug dose that is introduced into the human body. Therefore, the needs for analysing and controlling these systems are inevitable. Micro-pumps are an essential part in drug delivery systems for this purpose. Designing a micro-pump is a challenging task due to its important role. Nan-Chyuan Tsai [1] offers a fine review of different types of micro-pumps and of their mechanisms.

Typically, a piezoelectric micro-pump consists of a silicon membrane (S-membrane) which is actuated with a piezoelectric membrane (P-membrane) connected to it. By actuating the piezoelectric membrane in the resonant frequency, the highest efficiency can be achieved. Fig. 1 shows the schematic for a piezoelectric micro-pump.

Researchers have paid more attention to piezoelectric micro-pumps among all other types due to their controllability and reliability. Bart [2] worked on electrohydrodynamic (EHD) micro-pumps. This type of pumping uses the interaction of electric field and charges in the fluid to create the force for moving the fluid. Smits [3] modeled a piezoelectric micro-pump that was working peristaltically and had three valves. A fixed-valve micro-pump was designed and fabricated by Forster et al. [4]. Gerlach [5] designed and implemented a dynamic micro-pump with nozzle and diffuser as the inlet and outlet of the pump. He studied the dynamics of a fluid in the pump, and a static model for the membrane was derived. Olsson [6] fabricated a valveless micro-pump with double chamber. Das et al. [7] designed a control mechanism for controlling the flow of the micro-pump by modulating the electrostatic force. Johari [8] has designed a valveless piezoelectric micro-pump. However,

* Correspondence to: Automation and Robotic lab, Dept. of Mechanical Engineering, Amirkabir University of Technology (Tehran Polytechnic), Tehran, Iran. Tel.: +98 2164 543457.

E-mail address: mbahrami@aut.ac.ir (M. Bahrami).

http://dx.doi.org/10.1016/j.crme.2014.06.005

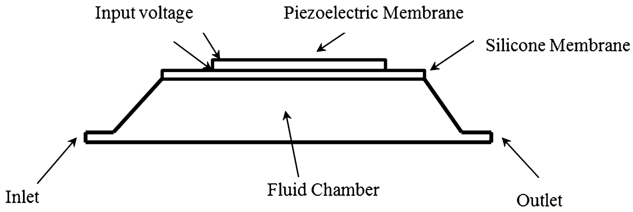

Fig. 1. Schematic view of a piezoelectric micro-pump [16].

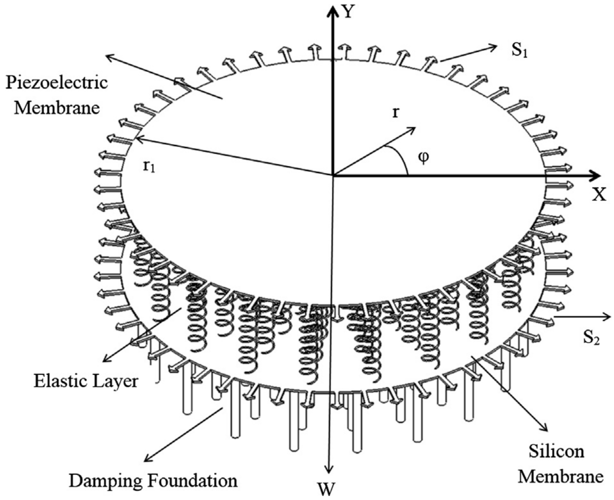

Fig. 2. Schematic view of the membrane in micro-pump.

the operation of this micro-pump has not yet been investigated theoretically in full detail. A software simulation with no theory has been reported in [9]. In lieu of all the works done on micro-pumps, it still remains to see the comprehensive model of the micro-pump for detailed analysis design purposes.

Ayela [10] modeled two membranes with a surrounding fluid. However, the two membranes were assumed as one with averaged mass. Energy methods and assumed mode shape were used to solve the problem. Cho et al. [11] modeled a two-layer membrane, one with piezoelectric material. Coupling has also been investigated, while a lumped parameter model is used to find the effect of the electromechanical coupling coefficient. Yih [12] used the pressure change in the micro-pump to derive the equations. Pan [13] modeled a micro-pump as only one membrane and added the effect of the piezoelectric membrane by importing an excitation force into the equation, and using thin plate theory to solve the problem. Oniszczuk [14] solved the problem of free and forced vibrations of a rectangular compound membrane. Noga [15] found the solution for the free transverse of a circular compound membrane. In both articles, the damping effect had been neglected.

Here, the piezoelectric micro-pump has been modeled as a two-membrane one, the membranes being elastically connected to each other. The damping effect of the fluid is added to the formulation as a viscose effect, related to the velocity of the membrane. An analytical solution has been attained for this model. Natural frequencies and mode shapes were calculated. Then orthogonality conditions have been discussed.

2. Dynamic model of the system

Fig. 2 shows the schematics of a circular double-membrane system. The membranes are assumed to be homogenous and are connected through a linear, massless elastic layer. The fluid has been assumed as a damping foundation beneath the silicon layer (not shown in this figure).

In this figure, r_1 is the radius of the membranes; S_1 and S_2 are the uniform constant tensions per unit length applied on the first and the second membrane, respectively, and w is the transverse of the membranes.

The system of equations for the system shown in Fig. 2 can be written as follows:

$$\begin{cases} m_1\ddot{w}_1 - S_1\Delta w_1 + k(w_1 - w_2) = f_1 \\ m_2\ddot{w}_2 - S_2\Delta w_2 + k(w_2 - w_1) + c\dot{w}_2 = f_2 \end{cases} \tag{1}$$

where w is a function of r, φ and t in polar coordinates. k is the stiffness coefficient of the elastic layer (elastic foundation of Winkler type between P- and S-membranes), and c is the damping coefficient of the fluid surrounding the second (silicon) membrane.

Also:

$$m_i = \rho_i h_i \tag{2}$$

$$\nabla w_i = \frac{\partial^2 w_i}{\partial r^2} + \frac{1}{r}\frac{\partial w_i}{\partial r} + \frac{1}{r^2}\frac{\partial^2 w_i}{\partial \varphi^2} \tag{3}$$

where ρ is the membrane density and h is the thickness of the membranes. It is assumed that each membrane is thin, homogeneous and perfectly elastic, and has constant thickness.

The membranes are fixed at their edges and the boundary, initial, and periodicity conditions are:

$$w_i(r_1, \varphi, t) = 0 \tag{4}$$

$$w_i(0, \varphi, t) < \infty \tag{5}$$

$$w_i(r, \varphi, t) = w_i(r, \varphi + 2\pi, t) \tag{6}$$

$$w_i(r, \varphi, 0) = w_{i0} \tag{7}$$

$$\left.\frac{\partial w_i}{\partial t}\right|_{(r,\varphi,0)} = v_{i0} \tag{8}$$

3. Solving the equations of motion

To find the natural frequency of the system, the homogenous part of the dynamic model of Eq. (1) is solved.

Using separation methods, the general solution of Eq. (1) will be as follows:

$$w_i(r, \varphi, t) = W_i(r, \varphi) T(t) \tag{9}$$

Based on the physical properties of the system, $T(t)$ can be written as:

$$T(t) = A\mathrm{e}^{\mathrm{j}\omega t} \tag{10}$$

where ω is the natural frequency of the system. Substituting (9) and (10) into (1) and simplifying the result, one can achieve the equations below:

$$\begin{cases} -m_1(\omega^2 W_1(r,\varphi)T(t)) - S_1(T(t)\Delta W_1) + k(T(t)(W_1 - W_2)) = 0 \\ -m_2(\omega^2 W_2(r,\varphi)T(t)) - S_2(T(t)\Delta W_2) + k(T(t)(W_2 - W_1)) + \mathrm{j}c\omega W_2 T(t) = 0 \end{cases} \tag{11}$$

Omitting $T(t)$ in Eq. (11) leads to:

$$\begin{cases} S_1 \Delta W_1 + (-k + m_1\omega^2) W_1 + k W_2 = 0 \\ S_2 \Delta W_2 + (-k + m_2\omega^2 - \mathrm{j}c\omega) W_2 + k W_1 = 0 \end{cases} \tag{12}$$

By eliminating W_2 from Eq. (11), Eq. (12) will be attained:

$$(\nabla + k_1^2)(\nabla + k_2^2) W_1 = 0 \tag{13}$$

where

$$\begin{aligned} k_{1,2}^2 = \frac{1}{2S_1S_2}\Big[&-(m_2S_1 + m_1S_2)\omega^2 + (S_2 + S_1)k + \mathrm{j}c\omega S_1 \\ &\pm \big\{-c^2\omega^2S_1^2 + 2S_2S_1k^2 + S_2^2m_1^2\omega^4 + S_1^2m_2^2\omega^4 + S_2^2k^2 + S_1^2k^2 \\ &- 2m_2\omega^2S_1^2k - 2\mathrm{j}m_2\omega^3S_1^2c + 2S_2^2m_1\omega^2k + 2\mathrm{j}kS_1^2c\omega - 2m_2m_1S_1S_2\omega^4 \\ &+ 2m_2S_1S_2k\omega^2 + 2m_1S_1S_2k\omega^2 + 2\mathrm{j}S_1S_2m_1c\omega^3 - 2\mathrm{j}S_1S_2kc\omega\big\}^{1/2}\Big] \end{aligned} \tag{14}$$

Again by using the technique of separation of variables, the solution of Eq. (13) is assumed:

$$W_1(r, \varphi) = R_1(r)\Phi(\varphi) \tag{15}$$

Substituting (14) into an equation of type (13):

$$(\nabla + k_i^2) W_1 = 0 \tag{16}$$

The following results will be achieved:

$$r^2R_1'' + rR_1' - \left(m^2 - (k_i r)^2\right)R_1 = 0 \tag{17}$$

$$\Phi'' + m^2\Phi = 0 \tag{18}$$

where $m = 0, 1, 2, \ldots$ and $i = 1, 2$.

The solution of Eqs. (17) and (18) is as follows:

$$R_{1im}(r) = P_{im} J_m(k_i r) + Q_{im} Y_m(k_i r) \tag{19}$$

$$\Phi_m(\varphi) = P_m \sin(m\varphi) + Q_m \cos(m\varphi) \tag{20}$$

where $J(.)$ and $Y(.)$ are the Bessel functions of the first and second kind, respectively.

Thus the mode shape function W_1 can be written as follows:

$$\begin{aligned} W_{1m}(r,\varphi) &= R_{1m}(r)\Phi_m(\varphi) = \Phi_m(\varphi)\sum_{i=1}^{2} R_{1im}(r) \\ &= \left[P_m \sin(m\varphi) + Q_m \cos(m\varphi)\right]\sum_{i=1}^{2}\left[P_{im} J_m(k_i r) + Q_{im} Y_m(k_i r)\right] \end{aligned} \tag{21}$$

By doing the same for W_2, and using Eq. (11):

$$\begin{aligned} W_{2m}(r,\varphi) &= R_{2m}(r)\Phi_m(\varphi) = \Phi_m(\varphi)\sum_{i=1}^{2} R_{2im}(r) \\ &= \left[P_m \sin(m\varphi) + Q_m \cos(m\varphi)\right]\sum_{i=1}^{2} d_i\left[P_{im} J_m(k_i r) + Q_{im} Y_m(k_i r)\right] \end{aligned} \tag{22}$$

where d_i is:

$$d_i = \frac{1}{k}\left(m_1\omega^2 - S_1\Delta + k\right) \tag{23}$$

or

$$d_i = \frac{1}{k}\left(m_1\omega^2 + S_1 k_i^2 + k\right) \tag{24}$$

Now, the boundary conditions can be applied to the solutions:

$$R_i(r) = 0 \tag{25a}$$

$$R_i(r) < \infty \tag{25b}$$

$$\Phi(\varphi) = \Phi(\varphi + 2\pi) \tag{25c}$$

By applying (25b), it can be shown that:

$$Q_{im} = 0, \quad i = 1, 2 \tag{26}$$

Hence, the following equations can be derived:

$$\begin{cases} P_{1m} J_m(k_1 r_1) + P_{2m} J_m(k_2 r_1) = 0 \\ d_1 P_{1m} J_m(k_1 r_1) + d_2 P_{2m} J_m(k_2 r_1) = 0 \end{cases} \tag{27}$$

or in matrix form:

$$\begin{bmatrix} J_m(k_1 r_1) & J_m(k_2 r_1) \\ d_1 J_m(k_1 r_1) & d_2 J_m(k_2 r_1) \end{bmatrix} \times \begin{bmatrix} P_{1m} \\ P_{2m} \end{bmatrix} = \begin{bmatrix} 0 \\ 0 \end{bmatrix} \tag{28}$$

In order to have a non-zero solution for coefficients P_{1m} and P_{2m} in Eq. (28), the following condition should be satisfied:

$$(d_1 - d_2) J_m(k_1 r_1) J_m(k_2 r_1) = 0 \tag{29}$$

It can be seen that $k_1 = k_2 = k_{mn}$. So, the characteristic equation is as follows:

$$J_m(k_{mn} r_1) = 0 \tag{30}$$

where n denotes the n-th root of the Bessel function and $n = 1, 2, \ldots$.

Solving Eq. (30) for k_{mn} and using Eq. (14) the frequency equation can be achieved. We use MAPLE software for this purpose.

The mode shapes of the first membrane can be expressed by the following equations:

$$W_{10n}(r,\varphi) = P_{10n} J_0(k_{mn} r) \tag{31}$$

$$W_{1mnc}(r,\varphi) = P_{1mnc} J_m(k_{mn} r)\cos(n\varphi) \tag{32}$$

$$W_{1mns}(r,\varphi) = P_{1mns} J_m(k_{mn} r)\sin(n\varphi) \tag{33}$$

And the mode shapes of the second membrane will be:

$$W_{20n}(r,\varphi) = d_i P_{10n} J_0(k_{mn} r) \tag{34}$$

$$W_{2mnc}(r,\varphi) = d_i P_{1mnc} J_m(k_{mn} r)\cos(n\varphi) \tag{35}$$

$$W_{2mns}(r,\varphi) = d_i P_{1mns} J_m(k_{mn} r)\sin(n\varphi) \tag{36}$$

for $m, n = 1, 2, \ldots$.

The orthogonality conditions write:

$$\begin{aligned}
\int_0^{r_1}\int_0^{2\pi} \rho W_{1mn}(r,\varphi) W_{1sl}(r,\varphi) r\mathrm{d}r\mathrm{d}\varphi &= \int_0^{r_1}\int_0^{2\pi} \rho W_{2mn}(r,\varphi) W_{2sl}(r,\varphi) r\mathrm{d}r\mathrm{d}\varphi \\
&= \rho \int_0^{2\pi} \sin(m\varphi)\sin(s\varphi)\mathrm{d}\varphi \times \int_0^{r_1} J_m(k_{mn} r) J_s(k_{sl} r) r\mathrm{d}r \\
&= \rho \int_0^{2\pi} \cos(m\varphi)\cos(s\varphi)\mathrm{d}\varphi \times \int_0^{r_1} J_m(k_{mn} r) J_s(k_{sl} r) r\mathrm{d}r \\
&= \begin{cases} 0, & m \neq s \text{ or } n \neq l \\ P^2_{mnc \text{ or } mns}, & m = s \text{ and } n = l \end{cases}
\end{aligned} \tag{37}$$

where P^2_{mn} is derived from normalization of the mode shapes, that is:

$$\int_0^{2\pi}\int_0^{r_1} \rho W_{1mnc \text{ or } 1mns}(r,\varphi) \mathrm{d}r\mathrm{d}\varphi \tag{38}$$

Hence:

$$P^2_{mnc} = P^2_{mns} = P^2_{mn} = \frac{2}{\pi\rho r_1^2 J^2_{m+1}(k_{mn} r_1)} \tag{39}$$

and

$$P^2_{10n} = \frac{1}{\pi\rho r_1^2 J_1^2(k_{0n} r_1)} \tag{40}$$

4. Finite-element modeling

The discrete models of the system under investigation are formulated using the finite element technique (ANSYS code). To find the first natural frequency and natural mode shape, the block Lanczos method is employed. The essential problem of this section is to build the FE model of the elastic and damping foundations.

The elastic foundation is modeled by a finite number of parallel massless springs. The stiffness modulus k_s of each spring can be obtained from Eq. (41) [15]:

$$k_s = \frac{k\rho_o}{b} \tag{41}$$

where ρ_o is the area of the membrane and b is the number of springs.

The spring-damper (ANSYS element combin) element, which is defined by two nodes, is used to realize the elastic layer. In this case, the damping capability of the elements is neglected.

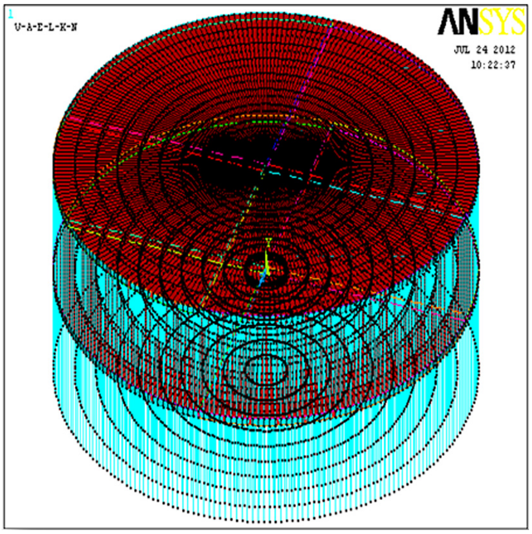

Fig. 3. Micro-pump model in ANSYS.

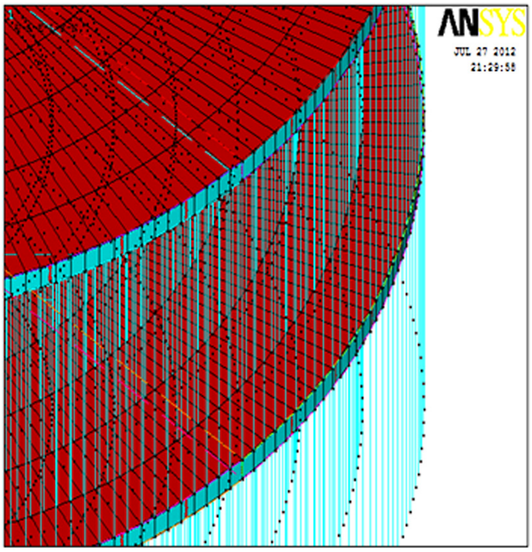

Fig. 4. Detailed view of the model. From top to bottom: piezoelectric layer, elastic layer, silicon layer and damping foundation as the fluid.

In order to model the damping effect of the fluid on silicon membrane in ANSYS, the damping foundation is modeled by a finite number of parallel massless dampers. The viscous damping coefficient c_{single} of each damper can be obtained from the relation:

$$c_{\text{single}} = \frac{c\rho_o}{b} \tag{42}$$

where ρ_o is the area of the membrane and b is the number of the dampers.

Again a spring-damper (combined) element is used to model the damping foundation. But in this case, the spring capability of element i is neglected. The four-node quadrilateral (shell63 & solid65) element is used to model the membrane. The boundary conditions are embedded as follows. All nodes lying on the edges of the membranes are simply supported with a possibility to slide freely in the radial direction.

The application of the constant tension is realized as each node lying on the outer edge is imposed by a concentrated tensile force in the radial direction.

The prepared model is consist of 2400 combined elements for the case of elastic foundation and 2400 combined elements for the one of damping foundation.

Figs. 3 and 4 show the micro-pump model in the ANSYS environment.

Table 1
Material properties of the micro-pump [16].

Silicon nitride (*Si3N4*)	
Mass density	2329 kg/mm^3
Modulus of elasticity	1.7×10^{11} N/mm^2
Poisson's ratio	0.3
Lead zirconate titanate (*PZT*)	
Mass density	7500 kg/mm^3
Shear modulus	9.5×10^9 N/mm^2
Poisson's ratio	0.31

Table 2
Parameters of the model.

S_1 $[\frac{N}{m}]$	S_2 $[\frac{N}{m}]$	k $[\frac{N}{m^3}]$	c $[\frac{kg}{s}]$
12.66	12.66	1×10^5	550

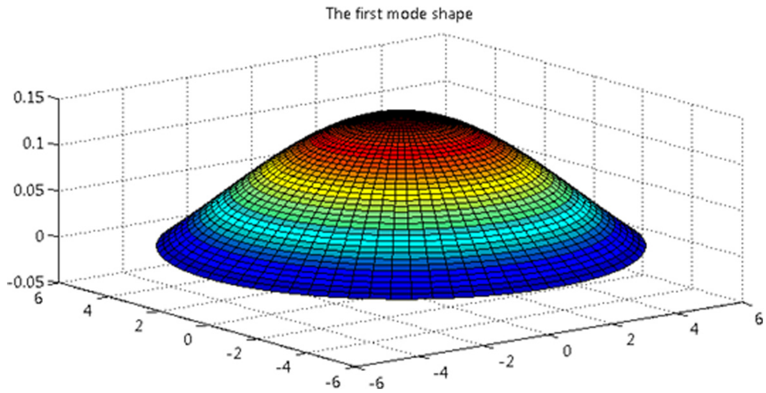

Fig. 5. First mode shape of membrane W_{201}.

5. Results

Some results are obtained using the simulation of a micro-pump with a radius of 2.5 mm and the thickness of 70 μm. The properties of the piezoelectric material and silicon are shown in Table 1.

Table 2 shows the values of tension forces on the edge of the membrane, the stiffness coefficient of the elastic layer and the damping coefficient of the fluid.

Since for a micro-pump only the first shape mode W_{201} and the natural frequency ω_{01} are needed, the parameters are achieved just for these values.

Using Eqs. (30) and (14), ω_{01} will have four possible values. Among these, two are too small and one is too large. So the only acceptable value is 3209.235 Hz.

Fig. 5 shows the first mode shape of membrane W_{201}.

For finite-element analysis the parameters are the same as the theoretical ones.

The result is shown in Fig. 6.

The functionality of the micro-pump is based on the first mode of the system. So it would be enough to compare just the first natural frequencies. The first natural frequency is $\omega_{01} = 3053.39$ Hz.

The absolute error will be obtained from the following equation:

$$\varepsilon_{01} = \frac{\omega_{01}^{\mathrm{f}} - \omega_{01}^{\mathrm{c}}}{\omega_{01}^{\mathrm{c}}} \times 100 \tag{43}$$

where ω_{01}^{f} and ω_{01}^{c} are the first natural frequency inferred from FE analysis and the theoretical solution, respectively. In this article, the absolute error will be:

$$\varepsilon_{01} = \frac{3053.39 - 3209.235}{3209.235} \times 100 = -4.85 \tag{44}$$

Therefore, the absolute error is about 4%, which is acceptable.

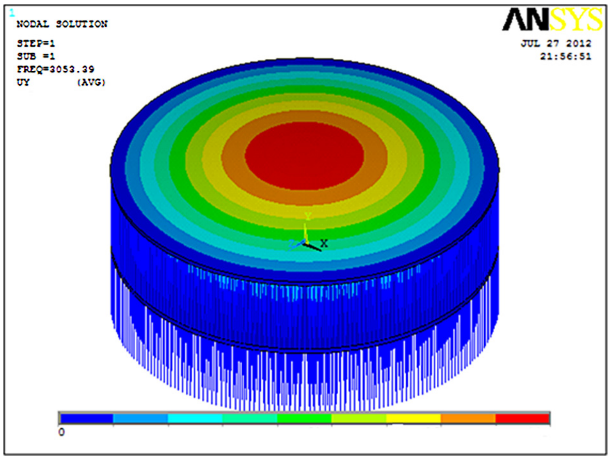

Fig. 6. ANSYS result for the micro-pump.

Comparing the results from ANSYS software and the explicit solution of the governing equations justifies our model of the micro-pump's diaphragm.

6. Conclusion

In this paper, a piezoelectric micro-pump diaphragm is modeled and analyzed. For this purpose, the micro-pump diaphragm is assumed to be a double-membrane one, consisting of piezoelectric and silicon materials that are connected by a massless, elastic, and linear layer. The damping effect of the fluid surrounding the silicon membrane is introduced into the equations. The systems of equations are solved analytically and the results applied in the case of a typical micro-pump. Natural frequency and mode shapes are derived and orthogonality conditions are discussed. To verify the model, finite-element analysis is developed. Since, for the functioning of the micro-pump, the first mode is required; only the first natural frequency is calculated and used for discussion and comparison. Although that, higher mode shapes are also attained. The results show a good compliance between the solution issued from theory and that from FE. The overall results show a good correspondence with the model developed by finite-element analysis.

References

[1] Nan-Chyuan Tsai, Chung-Yang Sue, Review of MEMS-based drug delivery and dosing systems, Sens. Actuators A 134 (2007) 555–564.
[2] S.F. Bart, et al., Microfabricated electrohydrodynamic pumps, Sens. Actuators A 21 (1–3) (1990) 193–197.
[3] J.G. Smits, Piezoelectric micropump with three valves working peristaltically, Sens. Actuators A 21 (1–3) (1990) 203–206.
[4] F. Forster, R. Bardell, M. Afromowitz, N. Sharma, Design, fabrication and testing of fixed-valve micropumps, in: Proceedings of the ASME Fluids Engineering Division, 1995 IMECE, vol. 234, 1995, pp. 39–44.
[5] T. Gerlach, H. Wurmus, Working principle and performance of the dynamic micropump, Sens. Actuators A, Phys. 50 (1–2) (1995) 135–140.
[6] A. Olsson, P. Enoksson, G. Stemme, E. Stemme, A valve-less planar pump in silicon, in: 8th International Conference on Solid-State Sensors and Actuators, and Eurosensors IX, Stockholm, 25–29 June, 1995, pp. 291–294.
[7] P.K. Das, S. Bhattacharjee, W. Moussa, Electrostatic force modulation as a flow control mechanism in microfluidic devices, in: International Workshop on System-on-Chip for Real-Time Applications, Banff, Canada, 2002.
[8] J. Johari, et al., Piezoelectric micropump with nanoliter per minute flow for drug delivery systems, Sains Malays. 40 (3) (2011) 275–281.
[9] U.F. González, Simulation of Mems Piezoelectric Micropump for Biomedical Applications, ALGOR, Inc., 2003.
[10] C. Ayela, L. Nicu, Micromachined piezoelectric membranes with high nominal quality factors in Newtonian liquid media: a Lamb's model validation at the microscale, Sens. Actuators B, Chem. 123 (2) (2013) 860–868.
[11] J. Cho, M. Anderson, R. Richards, D. Bahr, C. Richards, Optimization of electromechanical coupling for a thin-film PZT membrane: I. Modeling, J. Micromech. Microeng. 15 (2005) 1797–1803.
[12] Tachung C. Yih, T. Chiming Wei, B. Hammad, Modeling and characterization of a nanoliter drug-delivery MEMS micropump with circular bossed membrane, Nanomed. Nanotechol. Biol. Med. 1 (2005) 164–175.
[13] L.S. Pan, T.Y. Ng, G.R. Liu, K.Y. Lam, T.Y. Jiang, Analytical solution for the dynamic analysis of a valveless micro-pump—a fluid-membrane coupling study, Sens. Actuators A 93 (2001) 173–181.
[14] Z. Oniszczuk, Transverse vibrations of elastically connected rectangular double-membrane compound system, J. Sound Vib. 221 (2) (1999) 235–250.
[15] S. Noga, Free transverse vibration analysis of an elastically connected annular and circular double-membrane compound system, J. Sound Vib. 329 (2010) 1507–1522.
[16] ANSYS Tutorial, Example 4.4.